ON HEAT TRANSFER OF WEAKLY COMPRESSIBLE POWER-LAW FLOWS

by

Botong LI[a,b,c], Liangliang ZHU[c], Liancun ZHENG[d], and Wei ZHANG[a,b*]

[a] College of Mechanical Engineering, Beijing University of Technology, Beijing, China
[b] Beijing Key Laboratory for the Nonlinear Vibration and Strength of Mechanical Structures, Beijing University of Technology, Beijing, China
[c] International Center for Applied Mechanics, State Key Laboratory for Strength and Vibration of Mechanical Structures, School of Aerospace, Xi'an Jiaotong University, Xi'an, China
[d] Department of Mathematics and Mechanics, University of Science and Technology Beijing, Beijing, China

Original scientific paper
https://doi.org/10.2298/TSCI150701187L

This paper completes a numerical research on steady momentum and heat transfer in power-law fluids in a channel. Weakly compressible laminar fluids are studied with no slip at the walls and uniform wall temperatures. The full governing equations are solved by continuous finite element method. Three thermal conductivity models are adopted in this paper, that is, constant thermal conductivity model, thermal conductivity varying as a function of temperature gradient, and a modified temperature-gradient-dependent thermal conductivity model. The results are compared with each other and the physical characteristics for values of parameters are also discussed in details. It is shown that the velocity curve from the solution becomes straight at higher power-law index. The effects of Reynolds numbers on the dilatant fluid and the pseudo-plastic look similar to each other and their trends can be easily predicted. Furthermore, for different models, the temperature curves also present pseudo-plastic and dilatant properties.

Key words: *compressible flow, power-law fluid, thermal conductivity, heat transfer*

Introduction

Over the past few decades, the drag force behavior and energy transport of non-Newtonian fluid flows have attracted considerable attention. A prominent characteristic of non-Newtonian fluids is that their viscosity changes with shear rate. Several effective models have been proposed to depict this behavior of non-Newtonian fluids. Among these models, the so-called power-law model [1, 2], in which the shear stress varies according to a power-law function of the strain rate, has gained wide acceptance [3-5].

On the other hand, for nearly half a century, laminar flows of weakly compressible fluids have been investigated extensively due to their vast applications in many industrial processes involving gas flows at high speeds [6] or liquid flows in long channels (such as crude oil transport [7], and polymer extrusion [8]). An elaborative review of the literature shows that

* Corresponding author, e-mail: wzhang@bjut.edu.cn

weakly compressible flows have been investigated not only for Newtonian fluids [9-11] but also for non-Newtonian fluids, for example, the viscoelastic fluids [12].

However, there are far less works studying the weakly compressible power-law fluids. Thus, the present article is devoted to obtaining solutions for flows of weakly compressible power-law liquids in channels by adopting finite element method. Following the previous pioneering work [13], state equations are developed with isothermal compressibility considered. Both shear viscosity and thermal conductivity are assumed to be functions. Moreover, three different thermal conductivity models are considered, that is, constant thermal conductivity model, thermal conductivity varying as a function of temperature gradient, and a modified temperature-gradient-dependent model. And results of them are compared with each other.

Momentum governing equations

In the present work, we consider the steady, 2-D flow of a weakly compressible non-Newtonian power-law fluid under no slip at the walls. We assume that the bulk (or dilatational) viscosity is neglected and the viscosity is not constant but a function dependent on velocity gradient (the so-called power-law model [14-16]). Under these assumptions the continuity and the x- and y- components of the Navier-Stokes equations become:

$$\frac{\partial(\rho u)}{\partial x}+\frac{\partial(\rho v)}{\partial y}=0 \tag{1}$$

$$\rho\left(u\frac{\partial u}{\partial x}+v\frac{\partial u}{\partial y}\right)=-\frac{\partial p}{\partial x}+\frac{\partial}{\partial x}\left\{\mu\left[2\frac{\partial u}{\partial x}-\frac{2}{3}\left(\frac{\partial u}{\partial x}+\frac{\partial v}{\partial y}\right)\right]\right\}+\frac{\partial}{\partial y}\left[\mu\left(\frac{\partial u}{\partial y}+\frac{\partial v}{\partial x}\right)\right] \tag{2}$$

$$\rho\left(u\frac{\partial v}{\partial x}+v\frac{\partial v}{\partial y}\right)=-\frac{\partial p}{\partial y}+\frac{\partial}{\partial y}\left\{\mu\left[2\frac{\partial v}{\partial y}-\frac{2}{3}\left(\frac{\partial u}{\partial x}+\frac{\partial v}{\partial y}\right)\right]\right\}+\frac{\partial}{\partial x}\left[\mu\left(\frac{\partial u}{\partial y}+\frac{\partial v}{\partial x}\right)\right] \tag{3}$$

where ρ is the fluid density, u and v are the horizontal and transverse velocity components, respectively, and p is the pressure. The fluid density is supposed to obey a linear equation:

$$\rho=\rho_0[1+\beta(p-p_0)] \tag{4}$$

where β is the isothermal compressibility which is constant. Besides, the viscosity is assumed to be:

$$\mu=\mu_0\left[\sqrt{2\left(\frac{\partial u}{\partial x}\right)^2+2\left(\frac{\partial v}{\partial y}\right)^2+\left(\frac{\partial u}{\partial y}+\frac{\partial v}{\partial x}\right)^2}\right]^{n-1} \tag{5}$$

To non-dimensionalize the governing equations, we scale x by L, y by H, ρ by the reference density ρ_0, u by U, the transverse velocity v by UH/L, and the pressure p by μ_0U^n/L^n. For the sake of simplicity, in what follows, we will use the same symbols for all dimensionless variables.

$$\rho=1+\varepsilon p \tag{6}$$

$$\frac{\partial(\rho u)}{\partial x}+\frac{\partial(\rho v)}{\partial y}=0 \tag{7}$$

$$\mathrm{Re}\rho\left(u\frac{\partial u}{\partial x}+v\frac{\partial u}{\partial y}\right)=-\frac{\partial p}{\partial x}+\frac{\partial}{\partial x}\left(\Delta 2\frac{\partial u}{\partial x}\right)-\frac{2}{3}\frac{\partial}{\partial x}\left[\Delta\left(\frac{\partial u}{\partial x}+\frac{\partial v}{\partial y}\right)\right]+\frac{\partial}{\partial y}\left[\Delta\left(\frac{1}{\alpha^2}\frac{\partial u}{\partial y}+\frac{\partial v}{\partial x}\right)\right] \quad (8)$$

$$\alpha^2\mathrm{Re}\rho\left(u\frac{\partial v}{\partial x}+v\frac{\partial v}{\partial y}\right)=-\frac{\partial p}{\partial y}+\frac{\partial}{\partial y}\left(\Delta 2\frac{\partial v}{\partial y}\right)-\frac{2}{3}\frac{\partial}{\partial y}\left[\Delta\left(\frac{\partial u}{\partial x}+\frac{\partial v}{\partial y}\right)\right]+\frac{\partial}{\partial x}\left[\Delta\left(\frac{\partial u}{\partial y}+\alpha^2\frac{\partial v}{\partial x}\right)\right] \quad (9)$$

where

$$\Delta=\left[\sqrt{2\left(\frac{\partial u}{\partial x}\right)^2+2\left(\frac{\partial v}{\partial y}\right)^2+\left(\frac{1}{\alpha}\frac{\partial u}{\partial y}+\alpha\frac{\partial v}{\partial x}\right)^2}\right]^{n-1} \quad (10)$$

Here $\alpha=H/L$ is the aspect ratio of the channel, $\mathrm{Re}=\rho_0 L^n U^{2-n}/\mu_0$ is the Reynolds number and $\varepsilon=\beta\mu_0 U^n/L^n$ is the compressibility number.

The PDE (6)-(10) are supplemented by a system of non-dimensional boundary conditions:

$$u\Big|_{y=0}=0,\quad v\Big|_{y=0}=0,\quad u\Big|_{y=1}=0,\quad v\Big|_{y=1}=0,\quad u\Big|_{x=0}=1 \quad (11)$$

In the following, we solve the full governing equation by using the continuous finite element method which is defined.

Define the domain of our interest as $\Omega\subset R^2$. Denote the boundary of Ω by Γ which is sufficiently smooth. We may consider u and v in space Z, which is defined as $H^1(\Omega)$ if $n\le 1$ or $W^{1,n+1}(\Omega)$ if $n>1$, and p in $L^2(\Omega)$, see [17]. A weak formulation of eqs. (6)- (9) is to find u, v and p such that:

$$\int_\Omega\left\{\left[\frac{\partial(\rho u)}{\partial x}+\frac{\partial(\rho v)}{\partial y}\right]q\right\}\mathrm{d}\Omega=0\quad\forall q\in L^2(\Omega) \quad (12)$$

$$\int_\Omega\left\{\mathrm{Re}\rho\left(u\frac{\partial u}{\partial x}v_1+v\frac{\partial u}{\partial y}v_1\right)-\frac{\partial v_1}{\partial x}p+\frac{\partial v_1}{\partial x}\left(\Delta 2\frac{\partial u}{\partial x}\right)-\frac{2}{3}\frac{\partial v_1}{\partial x}\left[\Delta\left(\frac{\partial u}{\partial x}+\frac{\partial v}{\partial y}\right)\right]+\right.$$
$$\left.+\frac{\partial v_1}{\partial y}\left[\Delta\left(\frac{1}{\alpha^2}\frac{\partial u}{\partial y}+\frac{\partial v}{\partial x}\right)\right]\right\}\mathrm{d}\Omega=0\quad\forall v_1\in\mathrm{Z} \quad (13)$$

$$\int_\Omega\left\{\alpha^2\mathrm{Re}\rho\left(u\frac{\partial v}{\partial x}v_2+v\frac{\partial v}{\partial y}v_2\right)-\frac{\partial v_2}{\partial y}p+\frac{\partial v_2}{\partial y}\left(\Delta 2\frac{\partial v}{\partial y}\right)-\frac{2}{3}\frac{\partial v_2}{\partial y}\left[\Delta\left(\frac{\partial u}{\partial x}+\frac{\partial v}{\partial y}\right)\right]+\right.$$
$$\left.+\frac{\partial v_2}{\partial x}\left[\Delta\left(\frac{\partial u}{\partial y}+\alpha^2\frac{\partial v}{\partial x}\right)\right]\right\}\mathrm{d}\Omega=0\quad\forall v_2\in\mathrm{Z} \quad (14)$$

Based on a penalty or a sequential regularization formulation [18], eq. (12) can be replaced by the following:

$$\int_{\Omega}\left\{\left[\frac{\partial(\rho u)}{\partial x}+\frac{\partial(\rho v)}{\partial y}+\delta p\right]q\right\}\mathrm{d}\Omega=0 \quad \forall q\in L^2(\Omega) \tag{15}$$

where δ is a small penalty constant and we take $\delta=10^{-6}$ in our computations.

We use an iterative method to deal with the non-linear items in the governing equations:

$$\rho^{i-1}=1+\varepsilon p^{i-1} \tag{16}$$

$$\int_{\Omega}\left\{\left[\frac{\partial\left(\rho^{i-1}u^{i}\right)}{\partial x}+\frac{\partial\left(\rho^{i-1}v^{i}\right)}{\partial y}+\delta p^{i}\right]q\right\}\mathrm{d}\Omega=0 \tag{17}$$

$$\int_{\Omega}\left[\frac{u^{i}v_1-u^{i-1}v_1}{dt}+\mathrm{Re}\rho^{i-1}\left(u^{i-1}\frac{\partial u^{i-1}}{\partial x}v_1+v^{i-1}\frac{\partial u^{i-1}}{\partial y}v_1\right)-\frac{\partial v_1}{\partial x}p^{i}+2\Delta^{i-1}\frac{\partial u^{i-1}}{\partial x}\frac{\partial v_1}{\partial x}-\right.$$
$$\left.-\frac{2}{3}\Delta^{i-1}\left(\frac{\partial u^{i-1}}{\partial x}+\frac{\partial v^{i-1}}{\partial y}\right)\frac{\partial v_1}{\partial x}+\Delta^{i-1}\left(\frac{1}{\alpha^2}\frac{\partial u^{i-1}}{\partial y}+\frac{\partial v^{i-1}}{\partial x}\right)\frac{\partial v_1}{\partial y}\right]\mathrm{d}\Omega=0 \tag{18}$$

$$\int_{\Omega}\left[\frac{v^{i}v_2-v^{i-1}v_2}{dt}+\alpha^2\mathrm{Re}\rho^{i-1}\left(u^{i-1}\frac{\partial v^{i-1}}{\partial x}v_2+v^{i-1}\frac{\partial v^{i-1}}{\partial y}v_2\right)-\frac{\partial v_2}{\partial y}p^{i}+2\Delta^{i-1}\frac{\partial v^{i-1}}{\partial y}\frac{\partial v_2}{\partial y}-\right.$$
$$\left.-\frac{2}{3}\Delta^{i-1}\left(\frac{\partial u^{i-1}}{\partial x}+\frac{\partial v^{i-1}}{\partial y}\right)\frac{\partial v_2}{\partial y}+\Delta^{i-1}\left(\frac{\partial u^{i-1}}{\partial y}+\alpha^2\frac{\partial v^{i-1}}{\partial x}\right)\frac{\partial v_2}{\partial x}\right]\mathrm{d}\Omega=0 \tag{19}$$

where

$$\Delta^{i-1}=\left[\sqrt{2\left(\frac{\partial u^{i-1}}{\partial x}\right)^2+2\left(\frac{\partial v^{i-1}}{\partial y}\right)^2+\left(\frac{1}{\alpha}\frac{\partial u^{i-1}}{\partial y}+\alpha\frac{\partial v^{i-1}}{\partial x}\right)^2}\right]^{n-1} \tag{20}$$

Let $dt>0$ represents a time step size. $u^{i}=u(i\,dt,x,y)$ and $v^{i}=v(i\,dt,x,y)$ are obtained at time $i\,dt$. It does not have any effect to the previous equations although we add the *ghost* time to them because the velocity will not change any more when the steady-state is reached.

Next, we use a continuous finite element method to solve eqs. (16)- (20) with the help of the software FreeFem++, where we use the standard piecewise quadratic element for u,v and the piecewise linear element for the pressure, p.

Results and discussion

To study the effects of all parameters involved in the solution, *i. e.* the compressibility number, ε, the aspect ratio, α, and the Reynolds number we solve the full Navier-Stokes eqs. (16)-(20) with finite element method. Grid independence and validation of the code can be found in paper [19].

First of all, the effects of the power-law index n on the velocity components are illustrated in fig. 1. The difference of the velocity profile at $x=1.0$ (without special explanation, the

following drafts are all obtained at $x = 1.0$) relatively close to the exit is shown in fig. 1 for varying power-law index. While for low power-law index it is parabolic, the velocity curve from the solution becomes straight at higher power-law index. It is worth mentioning the case of $0 < n < 1$ is descriptive of pseudo-plastic non-Newtonian fluids while $n > 1$ describes dilatant non-Newtonian fluids.

In fig. 2, we show the velocity contours obtained with $\varepsilon = 0.05$, $\alpha = 0.5$ for two cases: (a) the dilatant fluid and (b) the pseudo-plastic. They look similar to their counterparts and their trends can be easily predicted. It is clear from the boundary condition that u is always positive and increases with the Reynolds number.

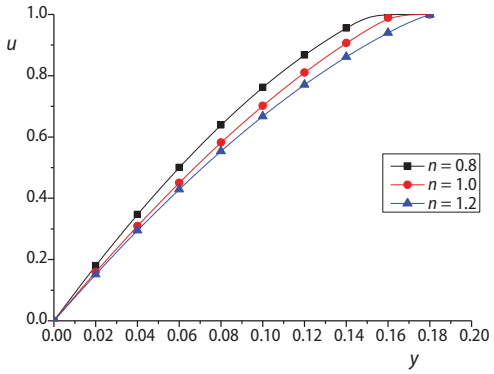

Figure 1. Comparison of velocity profiles with $\varepsilon = 0.05$, Re = 100, $\alpha = 0.5$

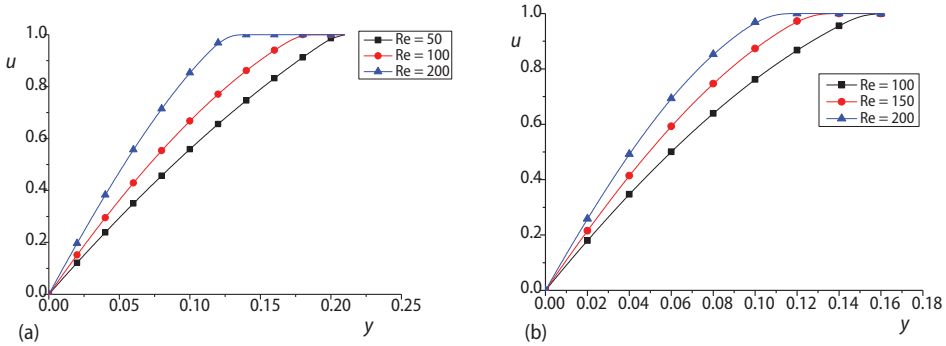

Figure 2. Effect of the Reynolds number on the velocity components; (a) $\varepsilon = 0.05$, $n = 1.2$, $\alpha = 0.5$, (b) $\varepsilon = 0.05$, $n = 0.8$, $\alpha = 0.5$

Pseudo-plastic fluids, another name for which is shear thinning fluids, include a certain number of complex solutions, such as lava, ketchup, whipped cream, blood, paint, and nail polish. It is also commonly found in polymer solutions and molten polymers. In this paper, we pay special attention on this kind of important fluids. The effects of the compressibility and the aspect ratio on the velocity components are illustrated in figs. 3(a) and 3(b), respectively. It can be observed that the profile flattens as compressibility is increased. In fig. 3(b), we show the velocity contours obtained with different shape of the channel. When the channel is relatively short ($\alpha = 1$), the flow is rather smoother than the case when the channel is long ($\alpha = 0.5$).

Energy equations

In this section, we present a research on steady heat transfer of power-law fluids by using different models of thermal conductivity. Three thermal conductivity models are shown in this paper. We focused on the effects of different models on the heat transfer of power-law fluids in the channel.

The energy equation studied now is as the form of:

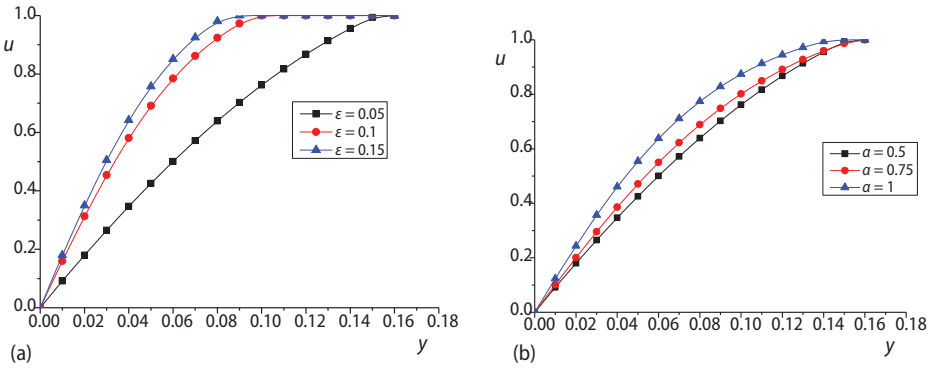

Figure 3. Effect of compressibility on the velocity components; (a) Re = 100, n = 0.8, α = 0.5, (b) Re = 100, n = 0.8, ε = 0.05

$$\rho c_p\left(u\frac{\partial T}{\partial x}+v\frac{\partial T}{\partial y}\right)=u\frac{\partial p}{\partial x}+v\frac{\partial p}{\partial y}+\frac{\partial}{\partial x}\left[k(T)\frac{\partial T}{\partial x}\right]+\frac{\partial}{\partial y}\left[k(T)\frac{\partial T}{\partial y}\right] \tag{21}$$

where c_p is the fluid specific heat, and $k(T)$ is the thermal conductivity function which is assumed to be as $k(T)=k_T[(\partial T/\partial x)^2+(\partial T/\partial y)^2]^{(tn-1)/2}$ (k_T is a positive constant). It is obvious that when $tn=1$, the model becomes the classical one with a constant thermal conductivity, when $tn=n$, the model is dependent on the thermal gradient which was proposed by Zheng *et al.* [20, 21], when $tn\neq n$, the second model is further investigated based on Fouriers law and the analogy between the velocity boundary-layer and the thermal one.

To non-dimensionalize eq. (21), we use the same dimensionless variable and scale T by T_0. Thus, the energy equation becomes:

$$\rho A\left(u\frac{\partial T}{\partial x}+v\frac{\partial T}{\partial y}\right)=u\frac{\partial p}{\partial x}+v\frac{\partial p}{\partial y}+B\frac{\partial}{\partial x}\left(\Gamma\frac{\partial T}{\partial x}\right)+\frac{B}{\alpha^2}\frac{\partial}{\partial y}\left(\Gamma\frac{\partial T}{\partial y}\right) \tag{22}$$

where

$$\Gamma=\left[\sqrt{\left(\frac{\partial T}{\partial x}\right)^2+\frac{1}{\alpha^2}\left(\frac{\partial T}{\partial y}\right)^2}\right]^{tn-1} \tag{23}$$

$$A=\frac{\rho_0 c_p T_0 L^n}{\mu_0 U^n} \tag{24}$$

$$B=\frac{k_T T_0^n}{\mu_0 U^{n+1}} \tag{25}$$

with the thermal boundary conditions:

$$T\big|_{y=0}=0,\quad T\big|_{y=1}=0,\quad T\big|_{x=1}=1 \tag{26}$$

Define the domain of T in W, which is defined as $W^{1,4}(\Omega)$ if $n\leq 3$ or $W^{1,n+1}(\Omega)$ if $n>3$. An iterative weak formulation of eq. (22) is to find T such that:

$$\int_{\Omega}\left[\frac{T^i v_3 - T^{i-1} v_3}{dt} + A\rho^{i-1}\left(u^i \frac{\partial T^{i-1}}{\partial x} v_3 + v^i \frac{\partial T^{i-1}}{\partial y} v_3\right) - u^i \frac{\partial v_3}{\partial x} p^i - v^i \frac{\partial v_3}{\partial y} p^i + \right.$$

$$\left. + B\Gamma^{i-1} \frac{\partial T^{i-1}}{\partial x}\frac{\partial v_3}{\partial x} + \frac{B}{\alpha^2}\Gamma^{i-1}\frac{\partial T^{i-1}}{\partial y}\frac{\partial v_3}{\partial y}\right] d\Omega = 0 \quad \forall v_3 \in Z \tag{27}$$

where

$$\Gamma = \left[\sqrt{\left(\frac{\partial T^{i-1}}{\partial x}\right)^2 + \frac{1}{\alpha^2}\left(\frac{\partial T^{i-1}}{\partial y}\right)^2}\right]^{tn-1} \tag{28}$$

Also, $T^i = T(i\,dt, x, y)$ are obtained at time $i\,dt$ and a continuous finite element method to solve energy equation with the help of the software FreeFem++, where we use the standard piecewise quadratic element for T.

Comparison and discussion

Figure 4 compares the different solutions obtained by using different models. The curves with $tn = 1.0$ are classical results with a constant thermal conductivity, the profiles with $tn = n$ are results with the thermal conductivity assumed to be a function of temperature gradient and the curves with $tn \neq n$ are results for a much more flexible model than the second one. With different models, the temperature curves also present pseudo-plastic ($0 < tn < 1$) and dilatant ($tn > 1$) properties.

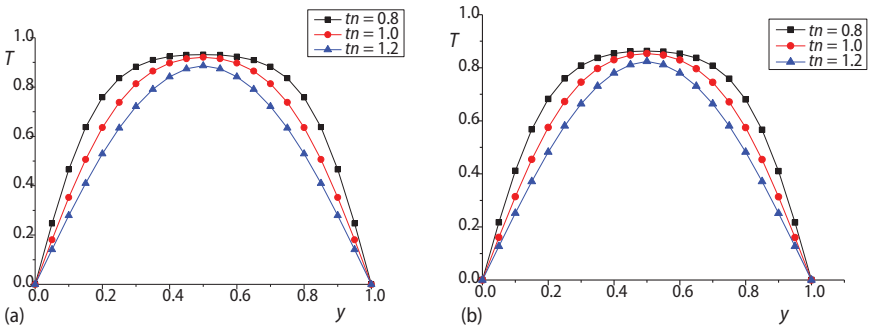

Figure 4. Comparison of temperature profiles between models; (a) Re = 100, α = 0.5, A = 150, B = 10, n = 0.8, ε = 0.05, (b) Re = 100, α = 0.5, A = 150, B = 10, n = 1.2, ε = 0.05

Figure 5(a) displays the dimensionless temperature profiles of different type of power-law fluids with constant thermal conductivity. Note in fig. 3(a) that the dimensionless temperature increases as the power-law index increases. In fig. 3(b), the temperature increases towards the rise of the compressibility. The thermal wave of the inlet temperature has less penetration near the center with the decreasing compressibility. It is a known fact that different values of n implies tremendous change in temperature.

Finally, fig. 6 shows the temperature profiles of pseudoplastic fluids ($n = 0.8$) obtained with $n = tn$. The shape in fig. 6(a) is rather flat in comparison with curves in other figures. Besides, it is really interesting to find out that fig. 6(b) seems to be of identical shape to fig. 5(b).

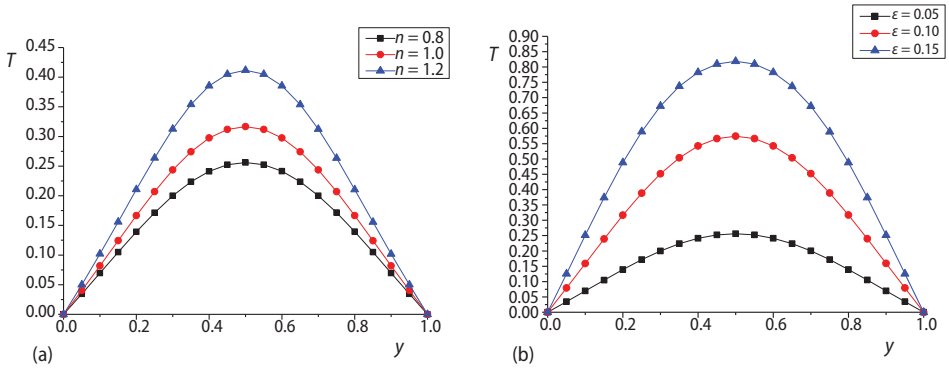

Figure 5. Temperature profiles with constant thermal conductivity model and different power-law indexes; (a) Re = 100, $\alpha = 0.5$, $A = 100$, $B = 10$, $tn = 1.0$, $\varepsilon = 0.05$, (b) Re = 100, $\alpha = 0.5$, $A = 100$, $B = 10$, $tn = 1.0$, $n = 0.8$

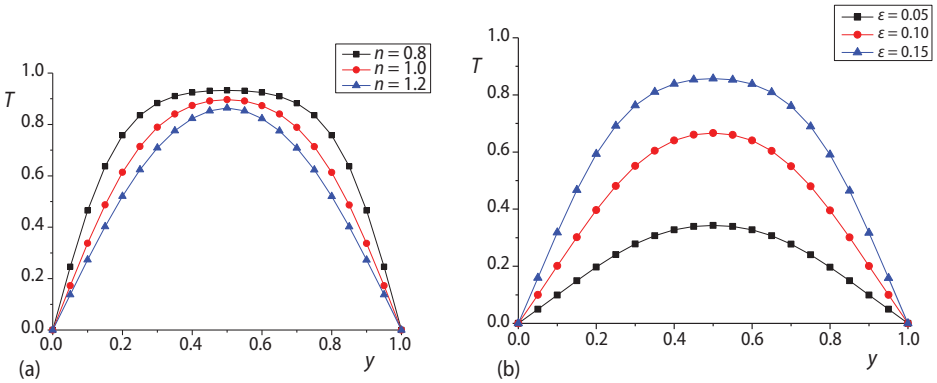

Figure 6. Temperature profiles with $n = tn$ and different power-law indexes; (a) Re = 100, $\alpha = 0.5$, $A = 200$, $B = 10$, $\varepsilon = 0.05$, (b) Re = 100, $\alpha = 0.5$, $A = 100$, $B = 10$, $n = 0.8$

Conclusions

This paper presents numerical studies on the problem of steady momentum and heat transfer of power-law fluids in a channel with weakly compressible property. Different thermal conductivity models are used and results of them are compared with each other. Some of the important findings of the paper are as follows.

- The velocity curve from the solution becomes straight at higher power-law index. The effects of Reynolds numbers on the dilatant fluid and the pseudo-plastic look similar to each other and their trends can be easily predicted.
- In the case of pseudoplastic fluids ($n = 0.8$), it can be observed that the profile flattens as compressibility is increased. And when the channel is relatively short the flow is rather smoother than the case when the channel is long.
- With different models, the temperature curves also present pseudo-plastic and dilatant properties.
- With a constant thermal conductivity model, the dimensionless temperature increases with the power-law index. Furthermore, the thermal wave of the inlet temperature has less penetration near the center with the decreasing compressibility.

Further studies will be focused on the determination of the thermal conductivity function of different fluids. Experiments will be designed to find out the exact changing patterns of the thermal conductivity function of a certain fluid flow.

Acknowledgment

The work is supported by the National Natural Science Foundation of China (11402188), the Fundamental Research Funds for the Central Universities (08143047) (2014gjhz16), and the Natural Science Basic Research Plan in Shaanxi Province of China (Program No.2015JQ1018).

Nomenclature

c_p – fluid specific heat, [Jkg^{-1}K^{-1}]
dt – time step size, [–]
H – channel height, [m]
k – thermal conductivity, [Wm^{-1}K^{-1}]
L – length of the wall, [m]
n – power law index, [–]
p – pressure, [Pa]
R – radius, [m]
Re – Reynolds number (= $\rho_f H^n U_0^{2-n}/\mu_f$), [–]
T – temperature, [K]
U – velocity for $y = \infty$, [ms^{-1}]
u, v – velocity components along x- and y-directions, respectively, [ms^{-1}]
x, y – Cartesian co-ordinates along the plate and normal to it, respectively, [m]

Greek symbols

α – aspect ratio of the channel (= H/L), [–]
β – isothermal compressibility, [–]
δ – penalty constant, [–]
ε – compressibility number, [–]
μ – dynamic viscosity, [Pas]
ρ – density of fluid, [kgm^{-3}]
Ω – calculation domain, [–]

Subscript

0 – refers to the inlet conditions

References

[1] Schowalter, W., The Application of Boundary-Layer Theory to Power-Law Pseudoplastic Fluids: Similar Solutions, *American Inst. Chem. Eng. J.*, *6* (1960), 1, pp. 24-28
[2] Acrivos, A., *et.al.*, Momentum and Heat Transfer in Laminar Boundary-Layer Flows of Non-Newtonian Fluids past External Surfaces, *American Inst. Chem. Eng. J.*, *6* (1960), 2, pp. 312-317
[3] Wang, T., Mixed Convection from a Vertical Plate to Non-Newtonian Fluids with Uniform Surface Heat Flux, *Int. Commu. Heat Mass Trans.*, *3* (1995), 22, pp. 369-380
[4] Wang, T., Mixed Convection Heat Transfer from a Vertical Plate to Non-Newtonian Fluids, *Int. J. Heat Fluid Flow*, *1* (1995), 16, pp. 56-61
[5] Hady, F., Mixed Convection Boundary-layer Flow of Non-Newtonian Fluids on a Horizontal Plate, *Appl. Math. Compu.*, *68* (1995), 2-3, pp. 105-112
[6] Venerus, D., Laminar Capillary Flow of Compressible Viscous Fluids, *J. Fluid Mech.*, *555* (2006), May, pp. 59-80
[7] Vinay, G., *et.al.*, Numerical Simulation of Weakly Compressible Bingham Flows: the Restart of Pipeline Flows of Waxy Crude Oils, *J. Non-Newtonian Fluid Mech.*, *136* (2006), 2-3, pp. 93-105
[8] Georgiou, G., The Time-Dependent, Compressible Poiseuille and Extrudate-Swell Flows of a Carreau Fluid with Slip at the Wall, *J. Non-Newtonian Fluid Mech.*, *109* (2003), 2-3, pp. 93-114
[9] Guo, Z., Wu, X., Compressibility Effect on the Gas Flow and Heat Transfer in a Microtube, *Int. J. Heat Mass Trans.*, *40* (1997), 13, pp. 3251-3254
[10] Georgiou, G., Crochet, M., Time-Dependent Compressible Extrudate-Swell Problem with Slip at the Wall, *J. Rheol.*, *38* (1994), 6, pp. 1745-1755
[11] Georgiou, G., Crochet, M., Compressible Viscous Flow in Slits with Slip at the Wall, *J. Rheol.*, *38* (1994), 3, pp. 639-654
[12] Belblidia, F., *et.al.*, Stabilised Computations for Viscoelastic Flows under Compressible Considerations, *J. Non-Newtonian Fluid Mech.*, *134* (2006), Mar., pp. 56-76
[13] Taliadorou, E., *et.al.,* Perturbation Solutions of Poiseuille Flows of Weakly Compressible Newtonian Liquids, *J. Non-Newtonian Fluid Mech.*, *163* (2009), 1-3, pp. 25-34

[14] Howell, T., *et.al.*, Momentum and Heat Transfer on a Continuous Moving Surface in Power Law Fluid, *Int. J. Heat Mass Trans.*, *40* (1997), 8, pp. 1853-1861
[15] Rao, J., *et.al.*, Momentum and Heat Transfer in a Power-Law Fluid with Arbitrary Injection/Suction at a Moving Wall, *Int. J. Heat Mass Trans.*, *42* (1999), 15, pp. 2837-2847
[16] Gorla, R., *et.al.*, Convective Wall Plume in Power-law Fluid: Second-order Correction for the Adiabatic Wall, *Warme-und Stoffubertragung, 27* (1992), 8, pp. 473-479
[17] Shi, H., *et.al.*, A Finite Element Method for Heat Transfer of Power-Law Flow in Channels with a Transverse Magnetic Field, *Math. Methods in the Appl. Sci.*, *37* (2014), 8, pp. 1121-1129
[18] Lin, P., Liu, C., Simulations of Singularity Dynamics in Liquid Crystal Flows: A CO Finite Element Approach, *J. Compu. Phys.*, *215* (2006), 1, pp. 348-362
[19] Li, B., *et.al.*, A Mixed Analytical/Numerical Method for Velocity and Heat Transfer of Power-Law Fluids with High Reynolds Number, *Nume. Math.: Theory Methods Applications*, *9* (2016), 3, pp. 315-336
[20] Zheng, L., *et.al.*, Heat Transfer of Power Law Non-Newtonian, *Chin. Phys. Lett.*, *23* (2006), 12, pp. 3301-3304
[21] Zheng, L., *et.al.*, Fully Developed Convective Heat Transfer for Power Law Fluids in a Circular Tube, *Chin. Phy. Lett.*, *25* (2008), 1, pp. 195-197

Paper submitted: July 1, 2015
Paper revised: November 19, 2015
Paper accepted: November 19, 2015